doi:10.1038/nature10095

Supplementary Information

1. Observational Details

PTF09atu was first detected by the 1.2 m Samuel Oschin Telescope on 2009 July 4 UT, three weeks before the PTF system was fully commissioned. PTF09atu is located at $\alpha = 16^h30^m24\overset{s}{.}55$, $\delta = +23°38'25\overset{''}{.}0$ (J2000). It was marked as a potentially interesting source on July 14, and photometric follow-up was performed on July 16 with the Palomar 1.5 m telescope in three bands. On July 29, we obtained a spectrum of PTF09atu with the 10 m Keck-I telescope. We requested *Swift* observations, which were performed on August 19. PTF09atu is marginally detected in the $uvw1$ band (AB mag $= 22.24 \pm 0.35$), but not significantly detected in the other UV bands.

PTF09cnd was first detected by PTF on 2009 July 13 UT. PTF09cnd is located at $\alpha = 16^h12^m08\overset{s}{.}94$, $\delta = +51°29'16\overset{''}{.}1$. It was marked as a potentially interesting source on August 7, and photometric follow-up was performed on August 11 with the Palomar 1.5 m telescope. On August 12, we obtained a spectrum of PTF09cnd with the 4.2 m William Herschel Telescope. We found the data similar to SN 2005ap and began an intensive follow-up program, which was partially hindered by wild fires in Southern California. We requested *Swift* observations, which began on August 18. PTF09cnd is well detected in all UV bands (AB magnitudes: $uvw2 = 19.81 \pm 0.05$, $uvm2 = 19.52 \pm 0.05$, $uvw1 = 18.99 \pm 0.04$, $u = 18.29 \pm 0.05$; these would be about 1.7, 1.7, 1.5, and 1.0 magnitudes brighter in the Vega system, respectively).

PTF09cwl was first detected by PTF on 2009 June 28 UT. PTF09cwl is located at $\alpha = 14^h49^m10\overset{s}{.}08$, $\delta = +29°25'11\overset{''}{.}4$. It was marked as a potentially interesting source on August 11. On August 25, we obtained a spectrum of PTF09cwl with the 10 m Keck-I telescope. We requested *Swift* observations, which were performed on August 29. PTF09cwl is well detected in all UV bands (AB magnitudes: $uvw2 = 22.72 \pm 0.32$, $uvm2 = 22.27 \pm 0.35$, $uvw1 = 20.99 \pm 0.15$, $u = 19.70 \pm 0.10$). After we posted a draft of this letter to the ArXiv preprint server, CRTS reported the detection of this same source to the IAU citing our work for needed confirmation[9]. Thus, PTF09cwl is also known by the IAU name, SN 2009jh.

PTF10cwr was first detected by PTF on 2010 March 5 UT. PTF10cwr is located at $\alpha = 11^h25^m46\overset{s}{.}67$, $\delta = -08°49'41\overset{''}{.}2$. It was marked as a potentially interesting source on March 14, and photometric follow-up was performed on March 17 with the Palomar 1.5 m telescope. On March 18, we obtained a spectrum of PTF10cwr with the 5.1 m Palomar Hale Telescope. We requested *Swift* observations, which began on March 19. PTF10cwr is well detected (AB magnitudes: $uvm2 = 19.97 \pm 0.05$, $uvw1 = 19.20 \pm 0.04$). CRTS independently detected[10] this source on March 13. After the CRTS and PTF results were reported in Astronomer's Telegrams on March 19 and 20, respectively, Pastorello et al. (ref. [12]) were able to recover the target as well from Pan-STARRS data obtained on March 12. Pastorello et al. further reported[13] the emergence of characteristic Type Ic supernova features to the IAU, and thus PTF10cwr is also known as SN 2010gx.

While each of the PTF events were detected with the*Swift* UV/Optical Telescope, we can only place limits on the x-ray flux from the *Swift* X-ray Telescope observations. The $0.2 - 10$ kev upper limits on PTF09atu, PTF09cnd, PTF09cwl, and PTF10cwr are 2×10^{44}, 6×10^{43}, 1×10^{44}, and 5×10^{43} erg s^{-1}, respectively. These upper limits are lower than the claimed X-ray detection[23] of SCP 06F6, which corresponds to 10^{45} erg s^{-1} at our redshift of $z = 1.189$. However, we remark that this measurement was made during a period of high background radiation.

Photometric measurements were extracted from the P48, P60, P200, and Keck data in circular apertures centered on the target with radii equal to the FWHM of point sources on the images (see Table S1). Zeropoints were calculated in reference to field stars calibrated by the SDSS. A similar analysis was performed for the Wise observations. For the *Swift* observations, we extracted aperture photometry following ref. 24. We make no corrections for line of sight reddening. Errors quoted account for formal (1-σ) uncertainties in the object and background sky only.

2. Details of the SYNOW Fit

The spectral synthesis code, SYNOW[21,25,26], was used to identify the line features in the combined (SCP 06F6, PTF, and SN 2005ap) spectra. This is a highly parametric code (free parameters include ion species, photospheric velocity, and the velocity distribution,

relative strength, and ion temperature of each individual ion assuming LTE), but it can be used to check for consistency in line identifications. The O II ion is found to produce line features quite similar to those seen near rest 4000 Å without introducing other, unwanted features. Thus, the identification of O II is secure. Similarly, C II, Si III and Mg II can account for the broad absorption bands in the UV. We do so using the same photospheric velocity, 15,000 km s^{-1} for all four ions, which further strengthens the identifications. However, detailed radiation transfer calculations (beyond the scope of this work) are required to verify the line identifications other than O II.

3. Lack of Hydrogen and Helium

A subtle P-Cygni profile can be seen near 6500 Å in the SN 2005ap spectra and is also present in the PTF sample. This feature has previously been identified[5] as Hα; however, later phase spectra of the PTF events do not show pronounced hydrogen features (see Figure S2). The late phase spectra instead indicate stripped envelope, or Type Ic, supernova (we note that previous Type Ic studies[27] identified the 6500 Å feature as C II $\lambda\lambda$6578, 6583; we favor this classification over hydrogen).

Some hydrogen poor supernovae show helium lines in their spectra (the Type Ib class). In these events, the helium atoms are thought to be excited by radioactive elements mixed into the ejecta.[28] The lack of helium signatures in the spectra presented here may thus indicate low levels of radioactive material mixed into the helium layers. Alternatively, the sample may be helium deficient. This later possibility is perhaps more likely since supernovae that explode with their envelopes intact (i.e. Type II events) typically show thermally excited helium lines at early times when radiation is still thermalized below the photosphere,[29] yet our sample shows no such features at comparable photospheric temperatures.

4. The Redshift of SCP 06F6

To determine the redshift of SCP 06F6, we first cross correlated each of the three spectra presented in ref. 6 against our spectra of PTF09atu, PTF09cnd, and PTF09cwl. The peak of the correlation function indicates a redshift of $z_{cc} = 1.21$. This would be the redshift

of SCP 06F6 if its broad spectral features were produced from ejecta moving with the same velocity and temperature fields as the PTF sample; however, we see from Figure 1 that the line features of SN 2005ap are $\sim$7,000 km s^{-1} faster than the PTF sample and there is a diversity of line profiles. We thus assume an error of 15,000 km s^{-1} for the cross correlation redshift.

Next, we searched for narrow Mg II doublet lines within this 15,000 km s^{-1} window. We fit two Gaussian profiles constrained to the same width to the narrow Mg II doublet in our PTF09cnd spectra to create a fitting template. From this, we determine the relative depths of the two lines, and the width. With these values and the spacing of the Mg II doublet held constant, we then scale and shift this template to determine the depth and redshift of the features in the combined SCP 06F6 spectra, which is made by removing broad features with a low order polynomial fit and adding all three spectra together. The best fit for the Mg II doublet template indicates a redshift of $z = 1.189$. This is $\sim$6,000 km s^{-1} slower than the cross correlation redshift.

We repeated this procedure on one million simulated datasets to determine the likelihood of noise troughs producing a bogus signal within the 15,000 km s^{-1} window that are as strong as the observed features. For each trial, we generated three simulated spectra with identical sampling to the SCP 06F6 spectra and convolved each of them so that their autocorrelation functions were similar to the observed data. We then register the spectra to the same wavelength bins through spline interpolation and add them together, just as the real data were combined. This ensures the correlated errors in adjacent bins are properly accounted for. We found that less than 0.13% of the trials produced features that were as strong or stronger than the actual observations. We therefore conclude that the Mg II doublet is detected in the combined SCP 06F6 data at the 3.0σ level, and that the redshift of SCP 06F6 is $z = 1.189$.

Previous studies have argued for a galactic origin,[30] redshifts of $z = 0.143$ (ref. 23 and 30), $z = 0.57$ (ref. 31), and the cluster redshift $z = 1.112$ (ref. 6). The redshift that we have determined argues against a physical association to the galaxy cluster.

5. PTF09cnd mass and kinetic energy

A lower limit on the kinetic energy of the emitting region of PTF09cnd is set by the observed radiated energy, 1.2×10^{51} erg. Since the radiating gas is moving at a velocity of $\sim 14,000$ km/s it implies a minimal mass of $M > \ M_{\odot}$.

An upper limit on the mass and kinetic energy in the emitting region is obtained by the requirement that the photon diffusion time from this region is shorter than the SN duration. The temperature of the radiating gas around the peak is $\sim 10^4$K and its radius is $R \sim 5 \times 10^{15}$ cm. This implies a density of $\sim 10^{-14} M/M_{\odot}$ gr cm^{-3}. The opacity at this density and temperature is $\kappa \approx 0.03$ cm^2/gr (http://opacities.osc.edu/rmos.shtml). This value is almost insensitive to the composition, namely the relative mix of C and O, as long as hydrogen and helium are absent. It is also weakly sensitive to the exact density. The opacity of the ejecta at this time is $\tau \approx \kappa M/R^2 \approx 3M/M_{\odot}$. The diffusion time is then $t_{diff} \approx \tau R/c \approx 6M/M_{\odot}$ day. The requirement $t_{diff} < 50$ day implies $M \lesssim 10 M_{\odot}$ and $E_k \lesssim 2 \times 10^{52}$ erg.

The mass and energy of the radiating shell is therefore constrained to a narrow range, $1 \lesssim M \lesssim 10 M_{\odot}$ and 10^{51} erg $\lesssim E_k \lesssim 2 \times 10^{52}$ erg. This implies that the radiative efficiency is $> 10\%$, which in turn allows almost no room for adiabatic losses. We therefore conclude that the deposition of internal energy in the expanding shell must have taken place at a late time, at a radius that is not much smaller than 10^{15} cm.

6. Host Galaxies

The host galaxies have luminosities near or below that of the Large Magellanic Cloud suggesting that they may harbor stars of sub-solar metallicities. From pre-outburst Sloan Digital Sky Survey (SDSS) data and late-time Keck imaging, we can place limits on the PTF host galaxies of $M_V \gtrsim -19$, $\gtrsim -18$, and $\gtrsim -17$ mag for PTF09atu, PTF09cnd, and PTF09cwl, respectively. The host of PTF10cwr is possibly detected by the SDSS, and would have a similar luminosity to the host of SN 2005ap[1,30]. SCP 06F6 also does not show a host brighter than $\gtrsim -18$ mag. Narrow emission lines (presumably from the host galaxies) can be seen contaminating the spectra of the PTF transients in outburst (see

Figure 2; Figure S1). Such signatures of active star formation indicate the presence of massive stars in the host galaxies.

7. Estimated Rate

The Texas Supernova Search[33] discovered SN 2005ap in two years of operation, and just 18 Type Ia supernovae (SNe Ia), while PTF found three similar events along with 114 spectroscopically confirmed SNe Ia in its first months of operation. Correcting for the larger selection volume and visibility window of SN 2005ap like events, the volumetric rate is roughly $10^{-8}\,\mathrm{Mpc}^{-3}\,\mathrm{year}^{-1}$ at $z \approx 0.3$ (Quimby et al. in prep.), or less than 1 for every 10,000 core-collapse supernovae.[34] The relatively high discovery rates (one for every few dozen SNe Ia) raises the question, "how have these events gone undetected until now?" The answer may simply be that much like SCP 06F6, there have been prior detections but without the local analogs as supplied by PTF they have remained (often unpublished) mysteries.

---

23. Gänsicke, B. T., Levan, A. J., Marsh, T. R. & Wheatley, P. J. SCP 06F6: A Carbon-rich Extragalactic Transient at Redshift z sime 0.14? *Astrophys. J.* **697**, L129–L132 June 2009.

24. Poole, T. S., Breeveld, A. A., Page, M. J., Landsman, W., Holland, S. T. *et al.* Photometric calibration of the Swift ultraviolet/optical telescope. *Mon. Not. R. astr. Soc.* **383**, 627–645 January 2008.

25. Fisher, A. K. *Direct analysis of type Ia supernovae spectra.* PhD thesis THE UNIVERSITY OF OKLAHOMA 2000.

26. Branch, D., Baron, E. A. & Jeffery, D. J. in *Supernovae and Gamma-Ray Bursters* (ed K. Weiler) 47–75 2003.

27. Hatano, K., Maeda, K., Deng, J. S., Nomoto, K., Branch, D. *et al.* in *New Century of X-ray Astronomy* (ed H. Inoue & H. Kunieda) 244–245 2001.

28. Lucy, L. B. Nonthermal excitation of helium in type Ib supernovae. *Astrophys. J.* **383**, 308–313 December 1991.

29. Dessart, L., Blondin, S., Brown, P. J., Hicken, M., Hillier, D. J. *et al.* Using Quantitative Spectroscopic Analysis to Determine the Properties and Distances of Type II Plateau Supernovae: SN 2005cs and SN 2006bp. *Astrophys. J.* **675**, 644–669 March 2008.

30. Soker, N., Frankowski, A. & Kashi, A. Galactic vs. extragalactic origin of the peculiar transient SCP 06F6. *Nature* **15**, 189–197 February 2010.

31. Chatzopoulos, E., Wheeler, J. C. & Vinko, J. Modeling the Light Curve of the Transient SCP06F6. *Astrophys. J.* **704**, 1251–1261 October 2009.

32. Adami, C., Picat, J. P., Savine, C., Mazure, A., West, M. J. *et al.* Deep and wide field imaging of the Coma cluster: the data. *Astr. Astrophys.* **451**, 1159–1170 June 2006.

33. Quimby, R. M. *The Texas Supernova Search.* PhD thesis University of Texas, United States – Texas (2006).

34. Bazin, G., Palanque-Delabrouille, N., Rich, J., Ruhlmann-Kleider, V., Aubourg, E. *et al.* The core-collapse rate from the Supernova Legacy Survey. *Astr. Astrophys.* **499**, 653–660 June 2009.

35. Soderberg, A. M., Berger, E., Page, K. L., Schady, P., Parrent, J. *et al.* An extremely luminous X-ray outburst at the birth of a supernova. *Nature* **453**, 469–474 May 2008.

36. Gezari, S., Halpern, J. P., Grupe, D., Yuan, F., Quimby, R. *et al.* Discovery of the Ultra-Bright Type II-L Supernova 2008es. *Astrophys. J.* **690**, 1313–1321 January 2009.

37. Miller, A. A., Chornock, R., Perley, D. A., Ganeshalingam, M., Li, W. *et al.* The Exceptionally Luminous Type II-Linear Supernova 2008es. *Astrophys. J.* **690**, 1303–1312 January 2009.

38. Matheson, T., Filippenko, A. V., Li, W., Leonard, D. C. & Shields, J. C. Optical Spectroscopy of Type IB/C Supernovae. *Astron. J.* **121**, 1648–1675 March 2001.

39. Kasen, D., Heger, A. & Woosley, S. in *First Stars III* (ed B. W. O'Shea & A. Heger) 263–267 American Institute of Physics, March 2008.

Supplementary Acknowledgements

We thank the participants of the 2009 KITP conference on "Stellar Death," in particular R. Kirshner and A. V. Filippenko, S. Phinney. and J. S. Bloom for comments on

the manuscript, D. Polishook for contributing Wise observations, and the *Swift* Science Operations Team. Some of the data presented herein were obtained at the W.M. Keck Observatory, which is operated as a scientific partnership among the California Institute of Technology, the University of California and the National Aeronautics and Space Administration. The Observatory was made possible by the generous financial support of the W.M. Keck Foundation. The William Herschel Telescope is operated on the island of La Palma by the Isaac Newton Group in the Spanish Observatorio del Roque de los Muchachos of the Instituto de Astrofísica de Canarias. LAIWO, a wide-angle camera operating on the 1-m telescope at the Wise observatory, Israel, was built at the Max-Planck-Institute for Astronomy (MPIA) in Heidelberg Germany with the financial support from MPIA and grants from the German-Israel Foundation and from the Israel Science Foundation. We acknowledge support from the Israeli Science Foundation, a European Union Seventh Framework Programme Marie Curie IRG fellowship, the Benoziyo Center for Astrophysics, a research grant from the Peter and Patricia Gruber Awards, the William Z. and Eda Bess Novick New Scientists Fund at the Weizmann Institute, and the Weizmann-Minerva program. The National Energy Research Scientific Computing Center is supported under Contract No. DE-AC02-05CH11231. We acknowledge support from the US Department of Energy Scientific Discovery through Advanced Computing program under contract DE-FG02-06ER06-04.

Table S1: Photometric observations.

Name	MJD	Tel.	Filter	Mag	err
PTF09atu	55016.258	P48	R	20.81	0.20
PTF09atu	55025.258	P48	R	20.56	0.08
PTF09atu	55035.289	P48	R	20.67	0.08
PTF09atu	55035.389	P60	g	20.60	0.10
PTF09atu	55040.356	P60	g	20.50	0.07
PTF09atu	55050.234	P48	R	20.27	0.17
PTF09atu	55056.320	P48	R	20.41	0.26
PTF09atu	55058.219	P48	R	20.19	0.07
PTF09atu	55059.160	P60	g	20.37	0.04
PTF09atu	55059.163	P60	r	20.06	0.04
PTF09atu	55059.166	P60	r	20.14	0.05
PTF09atu	55060.211	P60	g	20.44	0.04
PTF09atu	55060.214	P60	r	20.03	0.04
PTF09atu	55060.216	P60	r	20.06	0.04
PTF09atu	55061.165	P60	g	20.46	0.03
PTF09atu	55061.168	P60	r	20.07	0.04
PTF09atu	55061.170	P60	r	20.04	0.04
PTF09atu	55062.158	P60	g	20.44	0.03
PTF09atu	55062.161	P60	r	20.09	0.04
PTF09atu	55062.163	P60	r	20.09	0.04
PTF09atu	55063.157	P60	g	20.44	0.03
PTF09atu	55063.160	P60	r	20.01	0.04
PTF09atu	55063.163	P60	r	20.09	0.04
PTF09atu	55063.254	P48	R	20.13	0.08
PTF09atu	55064.155	P60	g	20.47	0.04
PTF09atu	55064.158	P60	r	20.07	0.04
PTF09atu	55064.161	P60	r	20.06	0.05
PTF09atu	55066.154	P60	g	20.50	0.04
PTF09atu	55066.157	P60	r	20.08	0.05
PTF09atu	55066.160	P60	r	20.09	0.05
PTF09atu	55067.153	P60	g	20.51	0.03
PTF09atu	55067.156	P60	r	20.11	0.04
PTF09atu	55067.158	P60	r	20.05	0.04
PTF09atu	55068.188	P60	g	20.59	0.04
PTF09atu	55068.191	P60	r	20.16	0.05
PTF09atu	55068.193	P60	r	20.14	0.05
PTF09atu	55069.156	P60	g	20.53	0.04
PTF09atu	55069.159	P60	r	20.16	0.05
PTF09atu	55069.161	P60	r	20.14	0.05
PTF09atu	55124.119	P60	r	20.96	0.28
PTF09atu	55205.556	P200	r	22.73	0.09
PTF09cnd	55025.391	P48	R	20.63	0.21
PTF09cnd	55035.273	P48	R	20.33	0.09
PTF09cnd	55049.281	P48	R	19.06	0.08
PTF09cnd	55052.301	P48	R	18.95	0.05

Table S1: Photometric observations.

Name	MJD	Tel.	Filter	Mag	err
PTF09cnd	55054.347	P60	r	18.84	0.04
PTF09cnd	55056.273	P48	R	18.79	0.03
PTF09cnd	55059.151	P60	r	18.64	0.02
PTF09cnd	55059.153	P60	r	18.62	0.02
PTF09cnd	55060.201	P60	r	18.58	0.02
PTF09cnd	55060.204	P60	r	18.59	0.01
PTF09cnd	55061.155	P60	r	18.57	0.01
PTF09cnd	55061.158	P60	r	18.57	0.01
PTF09cnd	55061.289	P48	R	18.65	0.03
PTF09cnd	55062.149	P60	r	18.52	0.01
PTF09cnd	55062.151	P60	r	18.54	0.01
PTF09cnd	55062.164	P48	R	18.66	0.03
PTF09cnd	55063.148	P60	r	18.51	0.01
PTF09cnd	55063.150	P60	r	18.53	0.01
PTF09cnd	55064.146	P60	r	18.49	0.01
PTF09cnd	55064.148	P60	r	18.48	0.01
PTF09cnd	55066.145	P60	r	18.47	0.02
PTF09cnd	55066.147	P60	r	18.46	0.01
PTF09cnd	55067.144	P60	r	18.43	0.01
PTF09cnd	55067.146	P60	r	18.44	0.01
PTF09cnd	55067.246	P48	R	18.45	0.02
PTF09cnd	55068.143	P60	r	18.41	0.01
PTF09cnd	55068.145	P60	r	18.41	0.01
PTF09cnd	55069.142	P60	r	18.39	0.01
PTF09cnd	55069.145	P60	r	18.38	0.01
PTF09cnd	55081.750	Wise	R	18.29	0.04
PTF09cnd	55084.227	P48	R	18.39	0.03
PTF09cnd	55089.713	Wise	R	18.09	0.03
PTF09cnd	55098.715	Wise	B	18.47	0.09
PTF09cnd	55107.180	P60	B	18.57	0.07
PTF09cnd	55117.675	Wise	B	18.93	0.04
PTF09cnd	55123.147	P60	B	18.95	0.04
PTF09cnd	55124.113	P60	B	18.98	0.06
PTF09cnd	55128.500	Wise	B	19.24	0.08
PTF09cnd	55133.500	Wise	B	19.37	0.14
PTF09cnd	55137.135	P60	B	19.28	0.17
PTF09cnd	55138.084	P60	B	19.68	0.14
PTF09cnd	55142.110	P60	B	19.64	0.09
PTF09cnd	55145.500	Wise	B	19.81	0.06
PTF09cnd	55181.510	P60	B	20.23	0.34
PTF09cnd	55183.508	P60	B	20.75	0.14
PTF09cnd	55185.498	P60	B	20.27	0.31
PTF09cnd	55189.490	P60	B	21.25	0.36
PTF09cnd	55192.479	P60	B	20.96	0.29
PTF09cnd	55201.484	P60	B	21.31	0.36

Table S1: Photometric observations.

Name	MJD	Tel.	Filter	Mag	err
PTF09cnd	55267.572	Keck	B	23.32	0.04
PTF09cwl	55010.633	P48	R	21.68	0.35
PTF09cwl	55021.277	P48	R	20.59	0.23
PTF09cwl	55034.234	P48	R	19.99	0.08
PTF09cwl	55050.199	P48	R	19.26	0.08
PTF09cwl	55081.227	Wise	R	19.13	0.10
PTF09cwl	55081.227	Wise	V	19.51	0.13
PTF09cwl	55205.540	P200	r	22.04	0.05
PTF09cwl	55267.602	Keck	g	25.33	0.07
PTF10cwr	55260.496	P48	R	19.73	0.24
PTF10cwr	55267.250	P48	R	19.16	0.04
PTF10cwr	55268.258	P48	R	18.85	0.03
PTF10cwr	55271.293	P48	R	18.76	0.03
PTF10cwr	55272.169	P60	r	18.57	0.04
PTF10cwr	55274.163	P60	r	18.52	0.04
PTF10cwr	55274.167	P60	B	18.48	0.06
PTF10cwr	55276.157	P60	r	18.63	0.04
PTF10cwr	55276.162	P60	B	18.65	0.07
PTF10cwr	55277.345	P60	r	18.60	0.03
PTF10cwr	55277.349	P60	B	18.54	0.05
PTF10cwr	55279.151	P60	r	18.53	0.10
PTF10cwr	55279.156	P60	B	18.82	0.12
PTF10cwr	55280.147	P60	r	18.62	0.10
PTF10cwr	55280.152	P60	B	18.78	0.13
PTF10cwr	55286.211	P60	r	18.60	0.11
PTF10cwr	55289.221	P60	B	18.74	0.05
PTF10cwr	55293.228	P60	r	18.64	0.05
PTF10cwr	55293.233	P60	B	18.98	0.06
PTF10cwr	55297.177	P60	r	18.73	0.03
PTF10cwr	55297.182	P60	B	19.14	0.04
PTF10cwr	55301.357	P60	r	18.79	0.03
PTF10cwr	55302.207	P60	B	19.42	0.16
PTF10cwr	55303.211	P60	r	18.92	0.03
PTF10cwr	55303.214	P60	B	19.48	0.05
PTF10cwr	55313.247	P60	r	19.26	0.13
PTF10cwr	55319.275	P60	r	19.53	0.07

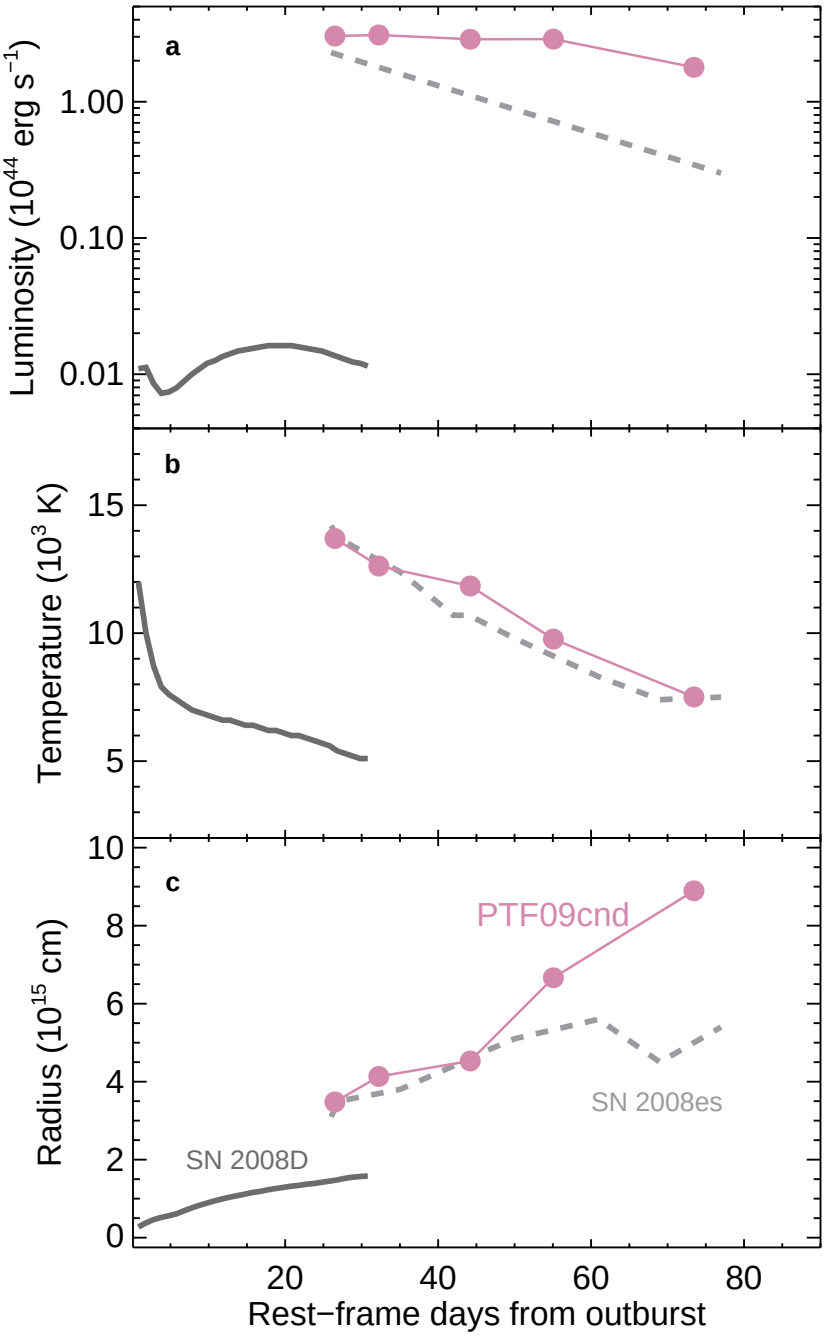

Figure S1. Radius, Temperature, and luminosity evolution of PTF09cnd. Purple dots give the values derived from black body fits to the *Swift* photometry, ground based g and r-band photometry, and spectra, as available. The *Swift* photometry is particularly import for the first four epochs when the spectral energy distribution peaks in the UV. For comparison we show the Type Ib SN 2008D, which was captured by *Swift* during shock breakout,[35] and the highly luminous Type II SN 2008es.[36,37] For both PTF09cnd and SN 2008es the actual phase is uncertain.

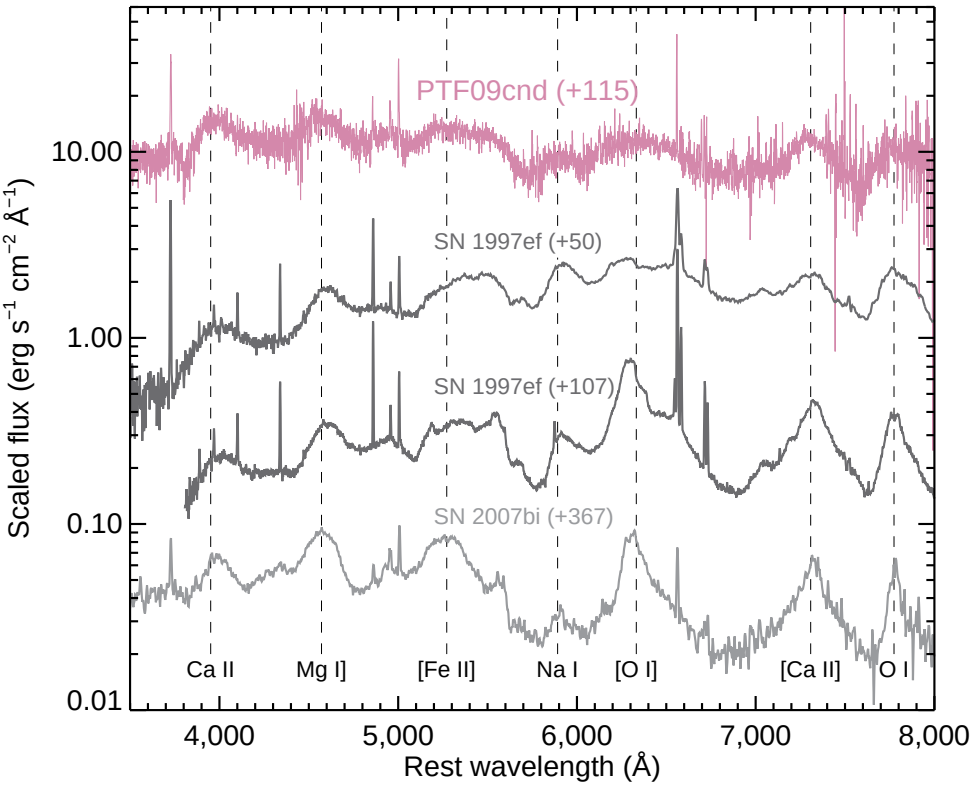

Figure S2. Pre-nebular spectra of PTF09cnd compared to two peculiar Type Ic supernovae. SN 1997ef may have been associated with a gamma-ray burst.[38] SN 2007bi was the first event found to be consistent with a pair-instability explosion[15]. Even though SN 1997ef was slow to enter the nebular phase in comparison to most Type Ic supernovae, the spectra obtained 50 rest frame days after V-band maximum are still more advanced than the spectra of PTF09cnd taken 115 (rest frame) days after V-band maximum. The forbidden [O I] $\lambda\lambda$6300,6364 doublet has not yet emerged in the PTF09cnd spectra, yet this feature is clearly present in the day 107 spectra of SN 1997ef. SN 2007bi also evolved slowly and its spectra were not fully nebular 367 rest frame days after its optical peak. For PTF09cnd, the Ca II H&K doublet shows a P-Cygni absorption plus emission profile, which indicates the photosphere persists. Narrow emission lines, which likely originate in the ionized interstellar gas of the host galaxies, can be seen in each case. Identifications[15] of the broad supernova features are shown below the SN 2007bi spectra.

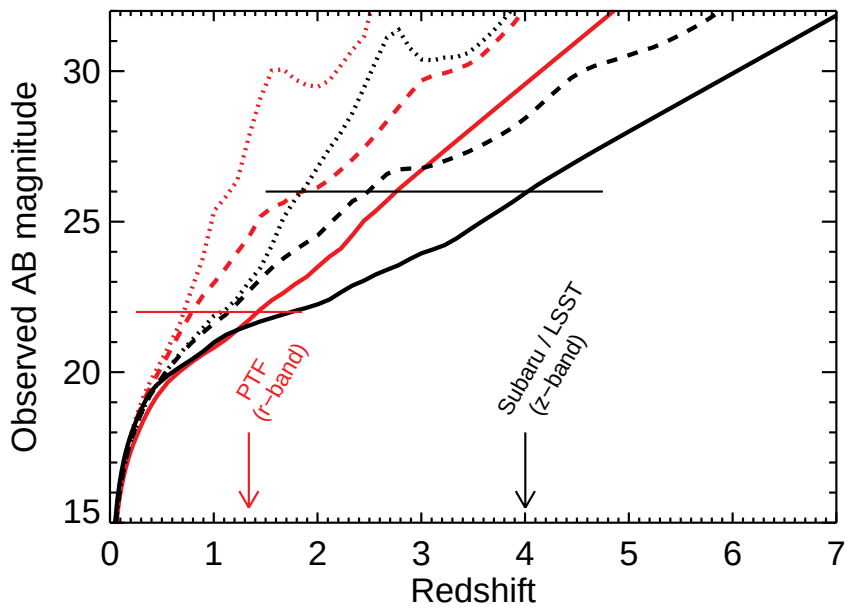

Figure S3. Detectability of luminous transients at large redshifts. The solid curves show the expected magnitude in the observer frame r-band (red) and z-band (black) as a function of redshift for SN 2005ap-like transients with an assumed absolute magnitude of -22 in the rest-frame r-band. For comparison, we have also plotted observed magnitudes derived from the pair-instability models of ref. 39 for both a solar (dotted lines) and a 10^{-4} solar (dashed lines) metallicity progenitor. In the PISN models, UV line blanketing increases with rising metallicity and thus the source flux rapidly diminishes as the *proper* UV photons are shifted into the observer bands. The SN 2005ap-like sample, however, shows relatively less UV absorption, which leads to comparably brighter sources at higher redshifts. Arrows mark the detection limits for the PTF r-band survey and for deep z-band surveys as could be done with Subaru or LSST.